

Article

Characteristics and Extent of Particulate Matter Emissions of a Ropeway Public Mobility System in the City Center of Perugia (Central Italy)

Beatrice Moroni ^{1,*}, Stefano Crocchianti ¹, Federica Bruschi ¹, Chiara Petroselli ¹, Alessandro Di Menno di Bucchianico ²,
Giorgio Cattani ², Luca Ferrero ³ and David Cappelletti ¹

- ¹ Dipartimento di Chimica Biologia e Biotecnologie, Università di Perugia, 06123 Perugia, Italy; croc@mail.dyn.unipg.it (S.C.); federica.bruschi@studenti.unipg.it (F.B.); petrosellichara@gmail.com (C.P.); david.cappelletti@unipg.it (D.C.)
- ² Istituto Superiore per la Protezione e la Ricerca Ambientale (ISPRA), 00144 Roma, Italy; alessandro.dimmenno@isprambiente.it (A.D.M.d.B.); giorgio.cattani@isprambiente.it (G.C.)
- ³ Dipartimento di Scienze dell'Ambiente e Territorio, Università di Milano Bicocca, 20126 Milano, Italy; luca.ferrero@unimib.it
- * Correspondence: beatrice.moroni1@posta.istruzione.it; Tel.: +39-075-5855529



Citation: Moroni, B.; Crocchianti, S.; Bruschi, F.; Petroselli, C.; Di Menno di Bucchianico, A.; Cattani, G.; Ferrero, L.; Cappelletti, D. Characteristics and Extent of Particulate Matter Emissions of a Ropeway Public Mobility System in the City Center of Perugia (Central Italy). *Atmosphere* **2021**, *12*, 1356. <https://doi.org/10.3390/atmos12101356>

Academic Editors: Daniela Cesari, Adriana Pietrodangelo, Dario Massabò and Daniele Contini

Received: 5 September 2021

Accepted: 14 October 2021

Published: 17 October 2021

Publisher's Note: MDPI stays neutral with regard to jurisdictional claims in published maps and institutional affiliations.



Copyright: © 2021 by the authors. Licensee MDPI, Basel, Switzerland. This article is an open access article distributed under the terms and conditions of the Creative Commons Attribution (CC BY) license (<https://creativecommons.org/licenses/by/4.0/>).

Abstract: Minimetrom (MM) is a ropeway public mobility system that has been in operation in the city of Perugia for about ten years to integrate with urban mobility and lighten vehicular traffic in the historic city center. The purpose of this work was to evaluate the impact of MM as a source of pollutants in the urban context, and the exposure of people in the cabins and the platforms along the MM line. These topics have been investigated by means of intensive measurement and sampling campaigns performed in February and June 2015 on three specific sites of the MM line representative of different sources and levels of urban pollution. Stationary and dynamic measurements of particle size distribution, nanoparticle and black carbon aerosol number and mass concentrations measurements were performed by means of different bench and portable instruments. Aerosol sampling was carried out using low volume and high-volume aerosol samplers, and the samples analysed by off-line methods. Results show that MM is a considerable source of atmospheric particulate matter having characteristics very similar to those of the common urban road dust in Perugia. In the lack of clear indications on road dust effect, the contribution of MM to the aerosol in Perugia cannot be neglected.

Keywords: urban aerosol; optical particle counters; miniDiSC; CPC; micro-aethalometer; SEM-EDS; ICP-MS; source profiles; road dust; combustive sources

1. Introduction

Urban mobility is the main source of atmospheric pollution in many urban contexts. Traffic-related emissions still provide about half the emissions of diesel particulate matter and NO_x [1], while black carbon (BC), PM_{2.5}, and ultrafine particles (UFP, particles with diameters <100 nm) are highly concentrated in the proximity of high-traffic roadways [2–4]. Exposure to traffic has been associated with adverse health effects including premature mortality, increased hospitalization, cardiac symptoms, lung cancer, hypertension, impaired respiratory health, and adverse pregnancy outcomes [5–8].

For years, urban mobility has been a challenge for urban air quality and health protection (e.g., [9]). Mobility affects all urban contexts, although its impact will vary according to the specific situation of the place, i.e., size of the city (e.g., [1,10,11]), its location with respect to local topography (e.g., [12,13]), weather and microclimate (e.g., [14]), type of the settlement and the mobility system (e.g., [1]), design details (e.g., [15]), synergy with other pollutants present in the urban context as well (e.g., industries, building heating systems, etc. [16,17]).

The problem of mobility in urban areas has been addressed in the framework of EU directives [18] through the development of Sustainable Urban Mobility Plans (SUMP; <http://www.eltis.org/mobility-plans/sump-online-guidelines>, accessed on 7 October 2021), via two complementary approaches: (i) managerial, regarding the causes and distribution of private mobility (e.g., management of congestion charges, encouraging car sharing and eco-driving practices), and (ii) infrastructural, affecting the typology and management of the public mobility system (e.g., means of transport, design of infrastructures). The success of the measures adopted seems to depend heavily on their coherence in the regional/local context [19]. In historic cities it is extremely important to manage both of these aspects to avoid congestion of spaces, especially in the case of the cities located on hills. There, in fact, one has to deal with the physical limits to traffic posed by narrow spaces, obligatory paths, location of public offices in respect to local and urban viability [20,21].

To address the problem of public mobility related to vehicular traffic, various non-road, non-exhaust public transport systems have been implemented. Light Rail Transit (LRT) systems constitute one of the most sustainable public transit modes given their high passenger capacity and low emissions of their electric vehicles. The use of LRT systems results in air quality benefits by reducing greenhouse gases on the streets [22] and in-vehicle pollutants exposure of the commuters [1]. However, the effects on air quality are greatly reduced if the infrastructures are located near busy roads [23]. A further issue, common to vehicular traffic and LRT systems, are non-exhaust emissions whose concentrations, exposure and health impact are still poorly measured and understood [9].

Perugia is the regional capital of Umbria (Central Italy). Like many other historic cities in Central Italy, it is located on a hill with its oldest part standing in the acropolis. The city center hosts most of the tourist attractions, which are popular with visitors from all over the world, and numerous public utility offices. This leads to a continuous flow of people moving into and from the city center daily. The result is traffic congestion at the access points during certain times of the day. Traffic is, actually, the main emission source in Perugia, accounting for approx. 40% of the total mass of PM_{10} , followed by biomass burning, urban soil and secondary sources, the three latter providing similar amounts in terms of PM_{10} mass fraction [24]. The Minimetron (MM) line was created in 2008 to address this problem. MM is a light cable-drawn transport system [25] consisting of small cabins driven by a wire rope continuously running at low speed on a steel track placed above the road level. The path runs on a radial transect, from a flat area to the top of the hill, passing through different areas in the town.

Due to its design and operating features, MM revealed itself a good mobile platform for real time monitoring and investigation of the dynamics of formation and dispersion of pollutants in the urban context [26–29]. In particular, the study by Crocchianti et al. [29] demonstrated the significant impact of traffic as the main source of stable pollution, and the role of atmospheric stability in the residence time of fine particles produced by traffic. Based on the statistical models a reduction of the fine particles of 13% was also found for a reduction of 50% of the number of vehicles passing over two main crossroads by the MM path. These results stimulate the development of an integrated public mobility system in which MM serves the mobility in the acropolis which is the part of the city most vulnerable to urban traffic.

To our knowledge there are no studies on the impact of similar transport systems in small cities like Perugia, as the only studies available for comparison refer to much more populated cities located in very different contexts [1,22,23]. The aim of this paper was to evaluate the impact of MM as a source of pollutants in the urban context, and the exposure of people in the cabins and the platforms along the MM line. These topics have been investigated by means of intensive measurement and sampling campaigns aimed at: (i) characterize the morphochemical features of particulate matter produced by MM (PM_{MM}), (ii) understand the dynamics of production and dispersion of PM_{MM} inside and outside the tunnels in the MM line, and (iii) establish the relevance of PM_{MM} within airborne

particulate matter in the city center of Perugia. The campaigns were conceived as part of a dedicated research project.

2. Materials and Methods

2.1. MM and the City

Perugia is the main city in Umbria. It is a medium-sized city with a population of about 170,000 inhabitants extending radially from the top of a hill over ~ 20 km². The MM line (Figure 1) connects the western suburb (~ 280 m a.s.l.) to the city center of Perugia (at ~ 450 m a.s.l.). It is an automatic transport system based on 20–25 rubber-tired cabins continuously running along a radial transect (~ 3 km) of the city on a steel track built 7 m above the road level. The path starts from a large suburban parking area, it crosses various heavy traffic roads and crossroads, passes through a park and above the main railway station, then it climbs Perugia hill and reaches the city center inside a 770 m long tunnel. There are seven stations along the path. While reaching a station, the cabins automatically detach from the rope and slow down until they stop due to the presence of vertical axle rubber wheels. The same braking system acts as an accelerator system when the cabins resume their run. The cabins have dimensions of $\sim 4 \times 1.5 \times 2.3$ m and move at variable speed throughout the day (15 to 25 km h⁻¹ from off-peak to rush hours, respectively) so as to cover the journey in a time span between 15 and 20 min. The car frequency at the stations, corresponding to the waiting time of travelers on the platform, does not exceed 5 min. Therefore the estimated duration of travelers' exposure to MM environment is less than 30 min at each ride. MM runs seven days a week, fourteen hours a day (from 7 a.m. to 9 p.m.).

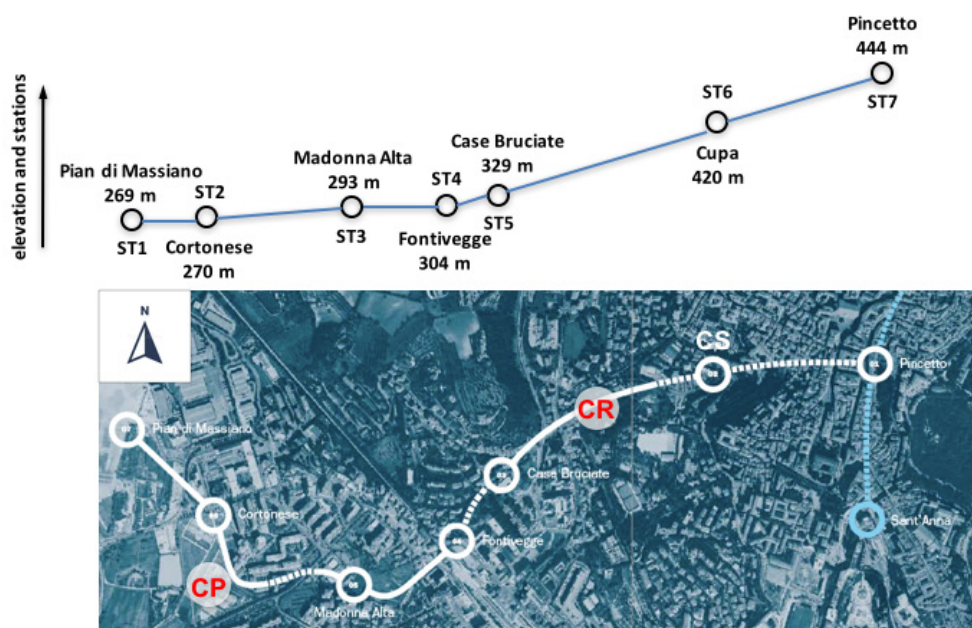


Figure 1. Path with elevation and stations of the MM line. Location of Cupa Station (CS), Cortonese Park (CP) and Angeloni Street crossroad (CR) are marked in bold capital letters.

2.2. Intensive Campaigns

Two intensive measurement and sampling campaigns were carried out in February and June 2015. The winter campaign, held from 9 to 13 February, took place in a particularly cold period, with snowfall followed by atmospheric stability. The summer campaign, held from 15 to 19 June, took place in a period of atmospheric stability, and was affected by a weak Saharan intrusion event (PM_{10} and $PM_{2.5}$ peak values of 21 and 11 $\mu\text{g m}^{-3}$, for a

$PM_{2.5}/PM_{10}$ ratio of 0.52) on 15 and 16 June. We have thus present, in two weeks, all the meteorological and environmental variables which insist on the place as observed in [29].

Having to investigate the composition of the PM produced by MM in relation to urban aerosol, the campaigns involved a specific site of the MM line (Cupa station; CS) representative of the production of PM_{MM} , along with two other sites representative of different sources and of different levels of urban air pollution (CR and CP in Figure 1). In fact CS is indoors, well inside a tunnel but not far from a crossroad highly affected by traffic pollution (CR in Figure 1) while CP (Figure 1) is located above a city park and, thus, represents urban background. CS is equipped with a forced ventilation system, but is also affected by the presence of a large ventilation opening located about 150 m away and halfway from the entrance to the tunnel.

Particle size distribution, nanoparticle and black carbon aerosol number and mass concentration measurements were performed in the campaigns. Particle size distribution measurements were performed using three different optical particle counters, namely a model 1.107 monitor (GRIMM, Austria) consisting of 23 size bins from 0.25 to 10 μm , 1 min time resolution, a FAI Instruments (Roma, Italy) optical particle counter (22 size bins from 0.28 to 10 μm , 6 s time resolution), and a 3330 optical particle sizer (OPS, TSI, USA; 17 size bins from 0.30 to 10 μm , 6 s time resolution). The GRIMM monitor was fixed in CS while the FAI counter was fixed in a specific cabin used for the measurements. In this latter case, the particle counter was miniaturized to be hosted in the upper vane of the cabin with selective inlet placed on the roof of the cabin itself. The same counter was integrated with the cabin control software, which allowed to monitor and to log information on the cabin position along the path during time. The TSI 3330 was used to perform measurements in different locations and conditions. Typical set-ups for measurements are shown in Figure 2.



Figure 2. Settings and instrumentations for samplings (a,b), and for stationary (a,b) and dynamic (c,d) measurements.

Before use, the three instruments underwent a cross-measurement test to compare their performance in terms of sensitivity and response time, with good results [26]. Individual cross-measurement tests are also performed once per year after each re-calibration of the instruments. The precision resulting from the procedure as a whole is better than 20% in

the total grain size range of measurement. The concentration of black carbon (BC) was measured using a micro-aethalometer (microAeth AE51 MAGEE Scientific; time resolution 1 s) while the number concentration of nanoparticles (NPs) was measured by a miniDiSC (size range 10–300 nm; time resolution 1 s; [30]) and a CPC (CPC 3007 TSI; size range 10–300 nm; time resolution 6 or 60 s). The latter instruments underwent a cross calibration and control test before each use, with good results (precision better than 5%).

Online measurements took place under stationary and dynamic conditions. In the first case, the instruments were kept fixed in their position for the entire duration of measurement. In the second case, the measurements were carried out using instruments placed permanently or temporarily inside and/or outside the customized cabin while moving along the MM path. Measurements took place in stationary conditions at CS and, partly, at CP, and in dynamic conditions in the three sites of the MM line.

In addition to measurements, atmospheric aerosol sampling was also carried out. Sampling took place by means of a low-volume aerosol sampler (ECHO-PM, Tecora, Italy, $2.3 \text{ m}^3 \text{ h}^{-1}$). The sampler was located at CS next to the access point to the rail and cabins (Figure 2) and was operated with PM_{10} and $\text{PM}_{2.5}$ size impactors. Quartz (QM-A, Whatman) and polycarbonate ($2 \mu\text{m}$ pore size, Sterlitech) filters were employed for OC-EC and SEM-EDS determinations, respectively. Immediately after sampling the filters were transferred to the lab and there stored in freezer at $-18 \text{ }^\circ\text{C}$ until measurements.

Measurements and samplings were carried out continuously over 24 h or, they were performed at fixed time slots during the day (Table A1). This was in order to better investigate the nature and the trend of the pollutants over time inside CS throughout the day and/or at special times during the day (peak traffic hours, night closing hours of the MM line) in respect to the outside (CP, CR).

The main meteorological and environmental parameters for the two periods of intensive campaign are reported in Table 1. These data were collected at CP where a fixed environmental measurement station managed by the local environmental protection agency (ARPA Umbria) is in operation. The station hosts a series of meteorological (temperature, pressure, humidity, wind, rain, solar radiation) and gas (sulfur, carbon, nitrogen oxides, ozone) sensors along with PM analyzers (SWAM, FAI Instruments, Roma, Italy) and a PBL Mixing Monitor (FAI Instruments). This latter is a natural radioactivity sampler-meter that automatically determines the concentration of the short-lived decay products of Radon, contained in the atmospheric particulate matter, above the ground level. Since Radon emission from the subsoil can be considered constant in the scale range of a few kilometers and a few days, and since Radon does not undergo chemical transformations, the concentration of its decay products near the ground mostly depends on the intensity and evolution of atmospheric turbulent diffusion processes. The use of radon as atmospheric stability index was successfully applied in Italy through years as reported in Vecchi et al. [31], who clearly demonstrate the relationship between radon concentration and planetary boundary layer (PBL) height.

The generalities of the project and the details of the instruments employed are reported in [29,32].

Table 1. Mean values of meteorological and environmental parameters for the two periods of intensive campaign. Standard deviation in parentheses.

Parameter	9–13 February	15–19 June
T ($^\circ\text{C}$)	5.8 (4.9)	19.3 (4.5)
RH (%)	73.5 (11.3)	69.7 (13.5)
Wind speed (m s^{-1})	0.7 (0.6)	0.8 (0.6)
PM_{10} ($\mu\text{g m}^{-3}$)	32.5 (14.3)	13.7 (5.2)
$\text{PM}_{2.5}$ ($\mu\text{g m}^{-3}$)	23.1 (12.6)	9.3 (1.2)
$\text{PM}_{2.5}/\text{PM}_{10}$	0.69 (0.05)	0.74 (0.2)

2.3. Scanning Electron Microscopy (SEM)

SEM observations and microanalyses were performed on six PM₁₀ samples, three for each measurement campaign, taken at CS in the same time slots, namely, from midnight to 5 a.m., from 8 a.m. to 1 p.m., and from 3 to 8 p.m. (Table A1). The purpose was to examine the composition of the aerosol in the closing hours of the plant, during peak traffic hours, and in the vicinity of the evening hours, respectively.

The samples were prepared by cutting single portions (~10 mm × 10 mm) from the central part of the polycarbonate sampling filters and mounting them on to SEM aluminum stubs using double-sided carbon tape. The samples were finally coated with a 100–150 Å carbon film to provide electrical conductivity and prevent charge build-up during the exposure to the electron beam.

Scanning electron microscopy imaging was performed using a Supra 25 microscope (ZEISS) equipped with a field emission gun and a GEMINI column employed at 15 kV and variable magnification (500 to 350,000×) and signal collection to distinguish particle types and textural details. The instrument is also equipped with an X-ray dispersive spectrometer (EDS microanalysis system QUANTA X, coupled with ESPRIT software for data treatment). EDS spectra (spot size 5, working distance 8.5 mm) were collected for 90 s and the elemental composition obtained after standardless matrix correction provided by the ESPRIT software. Values lower than 0.1 wt% (SEM detection limit) were omitted.

2.4. Chemical Speciation

The total concentration of the investigated elements in the freshly collected filters was determined on the polycarbonate sampling filters by ICP-MS spectroscopy using a triple quadrupole ICP-MS 8900 system (Agilent, USA) equipped with a collision/reaction cell (CRC), connected to an SP4 autosampler. The cyclonic spray chamber was thermostated at 2.7 °C and followed by a quartz torch and Ni cones. The acquisition was performed at 1550 W of plasma RF power. Instrument parameters were optimized for best sensitivity in the whole mass range, minimum oxides (<1.5%) and double charges (<1.5%). The analytical method included 29 different elements and each one of them was analyzed with one or more tunings. The standards used for the calibration was the Periodic Table Mix 1 for ICP (-traceCERT, Sigma-Aldrich) and Plasma CAL, a custom standard prepared by SCP SCIENCE. The stability of the measurements was monitored by several internal standards.

The polycarbonate filters were cut in half with ceramic scissors, previously cleaned using ultrapure water (18.2 MΩ). The filter was then inserted inside a teflon liner together with 8 mL of nitric acid (69%) and 2 mL of hydrogen peroxide (30% Suprapur). All the reagents used during this preparation procedure had a high level of purity in order to avoid any type of contamination of the samples. In particular, the nitric acid employed in this digestion was obtained by two successive distillations of Suprapur nitric acid with a subclean PTFE acid purification system. The digestion was performed using a MARS 6 type digester (Microwave Accelerated Reaction System, CEM). A specific digestion method was applied which consisted of a single ramp in which the samples reached the temperature of 170 °C in 20 min; this temperature was kept constant for 15 min before starting the cooling phase.

After digestion, the samples were transferred into polyethylene tubes and the volume equalized to 50 mL. To be sure that the metals were all transferred in the tubes with the sample, the liner and the stopper were both washed with 2 mL of HNO₃ 0.5% (diluted from the same HNO₃ used during the digestion process). The samples were then made up to 25 mL with the same nitric acid solution, and finally diluted by a factor of 100, inside a tube with a 15mL capacity, using ultrapure water. Blank solutions were also prepared in the same way in order to check any possible contamination derived from the preparation procedure.

Elemental and organic carbon (EC and OC) in the PM_{2.5} CS samples were determined by thermal-optical transmittance (TOT, Sunset Laboratory Inc.TM, Tigard, OR, USA) using

the NIOSH protocol. Organic Matter (OM) was determined from OC using a factor 1.7 for remote places in Italy [33].

3. Results and Discussion

3.1. Size and Sources of PM

Trends of particle number concentration at CS for different size ranges in the timespans 9–13 February and 15–19 June are reported in Figure 3. In the graphs different size bins have been combined in order to make the data obtained using the two different particle counters employed in the campaigns (GRIMM and OPS; Table A1) comparable. For the same reason the 0.28–0.4 μm size range is reported in the only case of the winter campaign which is the one in which the GRIMM particle counter was employed.

All the curves show daily fluctuations of the size ranges. Fluctuations are much larger and more regular in winter. In that period two clear daily maxima, the first between 8 and 12 a.m. and the second between 6 and 12 p.m., are observed (Figure 3a). The comparison with the environmental parameters in the vicinity of the measurement station shows a clear correlation of the morning peak with traffic trends (Figure 3b), while the conformation of the evening peak suggests the combined effect of traffic and other sources of urban air pollution, likely domestic heating (Figure 3c). The background of measurements of fine particles (diameter less than 1.0 μm in size) also tends to rise regularly starting from February 12. In that period a condition of marked atmospheric stability was attained, well evidenced by the simultaneous, large oscillations of the atmospheric stability index (Radon measurements in Figure 3c). These observations confirm what Crocchianti et al. [29] found about the role of traffic and atmospheric stability on the concentration of fine particles, and also suggest the role of different polluting sources (e.g., domestic heating) on fine particle trends. In summer, the daily fluctuations in the concentration of particulate pollutants have a much more reduced and a more irregular trend, especially in the first two days of measurement. Furthermore, the concentrations of fine particles are much lower than those recorded in winter while the concentrations of coarse particles are higher by more than one order of magnitude. This effect was likely the result of concomitant: (i) lack of local emissions by domestic heating, (ii) dilution effect of local emissions by increasing height of the planetary boundary layer (PBL), and (iii) occurrence of the Saharan intrusion which, despite its weak intensity, introduced a sufficient quantity of dust to level the oscillations induced by local sources of pollution.

Some pattern distinction was also observed in the transition between the fine and the coarse particle size ranges. This consists in a reduction of the gap between the ridges and the valleys of the curves leading to a general flattening of the curves. Assuming the fine/very fine particle classes being related to combustion anthropogenic sources (mainly traffic), and the coarse/very coarse ones to MM emissions, this effect can be explained with the mixing between the two components. This is particularly evident in winter time, likely due to the low proportion of coarse to very coarse particles in respect to the fine and the very fine ones in this period.

All these observations reveal a dependence of the polluting particulate concentrations on both the emission sources (both urban and natural) and the environmental conditions (oscillation of the altitude of the PBL) even in the interior of the MM tunnel. After a three-years long period of measurements, Crocchianti et al. [29] found a statistically significant accumulation of fine particles during the week, from a minimum on Monday to a maximum on Friday, due to vehicular traffic. Looking to this point we can assume that the traffic contribution to the aerosol size distribution in the same day of the week be approximately constant or, at least, comparable.

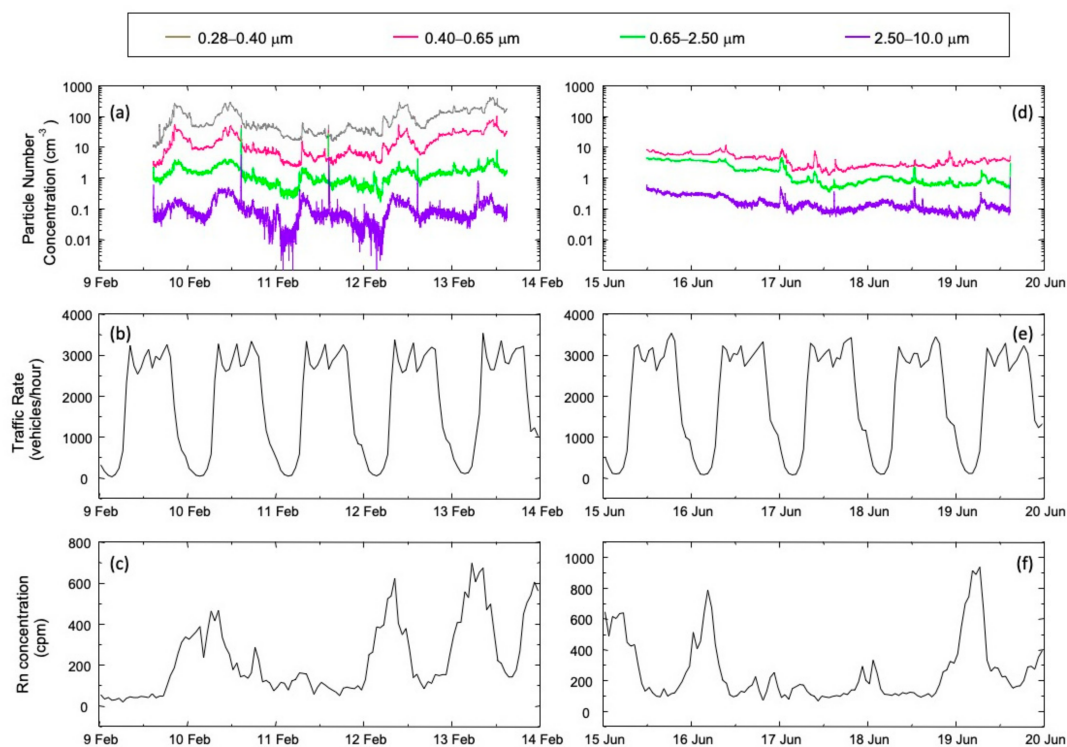


Figure 3. Trends of particle number concentration at CS for different size bins in the timespans 9–13 February (a) and 15–19 June (d) with corresponding traffic rates (b,e) and Atmospheric Stability Index (Radon concentration, (c,f)). The grey bars represent the MM operation time.

For this reason, and in order to verify the impact of MM in respect to traffic (this latter being the main emission source in Perugia), in Figure 4 we compare the particle size distributions at CS in different time spans of the same weekdays in February and June. The particle number concentrations are highest between 8 and 10 a.m., and lowest between midnight and 2 a.m., with the only exception on 16 and, especially, 17 June likely due to some additional wind transit and/or air mass movement within the tunnel itself (see Figure 3). The fact that the spread of data tends to be higher in the coarse than in the fine mode, and the fact that the coarse particle number concentrations are always lower when MM is not in operation, both point to the existence of a significant contribution to urban PM in Perugia by MM.

This is confirmed by a 96-h measurement test carried out in winter, in stationary conditions, in a different campaign (Appendix B) using two distinct optical particle counters working in pair, namely the OPS positioned at the side of the MM track, at eye level, and the GRIMM positioned below the rails (Figure 2a,b). The two data sets show similar trends, both characterized by three concentration maxima corresponding to the diameters of 0.65, 2 and 6–7 μm, with higher values of particle concentrations above the rails. This occurs either when the MM line is on or when it is off (Figure 5). However, some clear distinction is observed depending on sampling location and site operation, namely: (i) aerosol particle number concentrations are higher over the rail, (ii) number concentrations of fine particles are higher when MM is off, and (iii) number concentrations of coarse particles are higher when MM is on. This shows that MM is a source of coarse particles in itself, and that these particles tend to remain suspended in the air. This can be partly due to the air motion induced by the cabins in movement, but also to the existence, at CS, of an aeration system that tends to establish a circulation of air grazing the tracks, or above them, capable of keeping the particles present in the tunnel suspended, whether they are produced by the MM (mostly coarse particles) or coming from the outside (mostly fine-ultrafine particles).

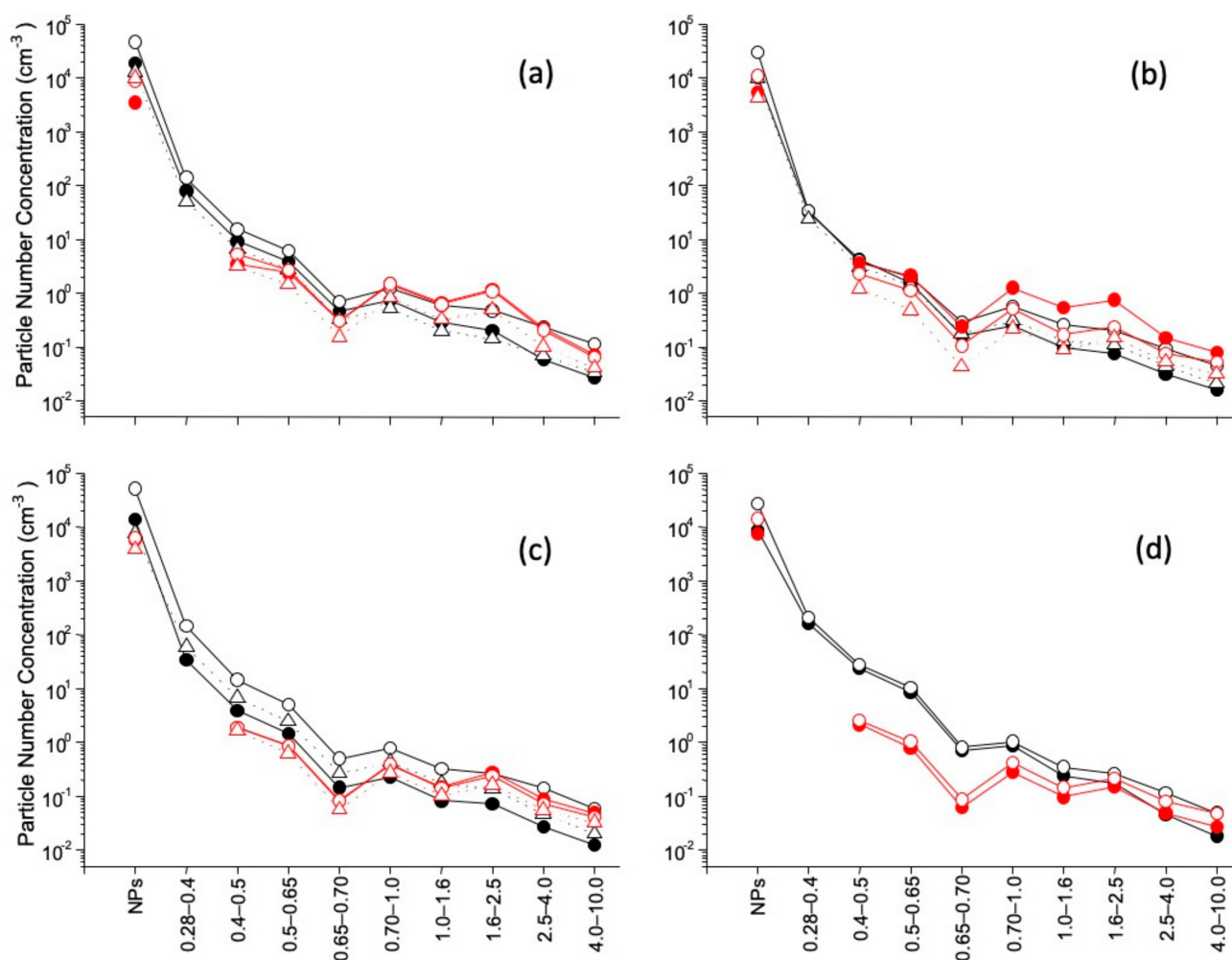


Figure 4. Particle number concentrations in the different size ranges (from nanoparticles, NPs, to 10 μm) and different time spans (solid circles, 00:00 to 02:00 a.m.; open circles, 08:00 to 10:00 a.m.; up triangles, 04:00 to 06:00 p.m.) at CS in the same weekdays in February (black symbols and lines) and June (red symbols and lines): (a) 10 February and 16 June; (b) 11 February and 17 June; (c) 12 February and 18 June; (d) 13 February and 19 June.

3.2. MM as a Source of PM

Results of SEM observations revealed two different particle types having MM as their source. The first type consists of rubber fragments. These particles have various shape and size and show the typical heterogeneous texture due to the presence of numerous inclusions immersed in a soft matrix (Figure 6a). The inclusions are micrometric to submicrometric in size and rounded in shape. Most of them are iron-rich metal oxides (with prevailing Fe along with variable amounts of Zn, Cu, Cr, Mn, Ni; Figure A1), others are silicates (mainly mica and feldspar grains; Figure A1), while some granules consist of barium sulfate. All these particles are ascribed to the fillers used to regulate and improve rubber properties such as wet grip and rolling resistance of the tire treads (e.g., [34–36]). Rubber is the most widespread material within the MM line as the tire tread of the wheels of both the cabins and the braking system are made of rubber. Rubber tires are also the main yearly MM consumable, due to the tire wear. Therefore tire wear seems to be the main emission source related to the operation of MM. A great number of filler particles released by the rubber are also found suspended in the air, thus determining a fine to very fine grained secondary aerosol enriched in Fe (e.g., Figure 6b), silicates and sulfates. Representative bulk chemical analyses of rubber particles are reported in Table A2.

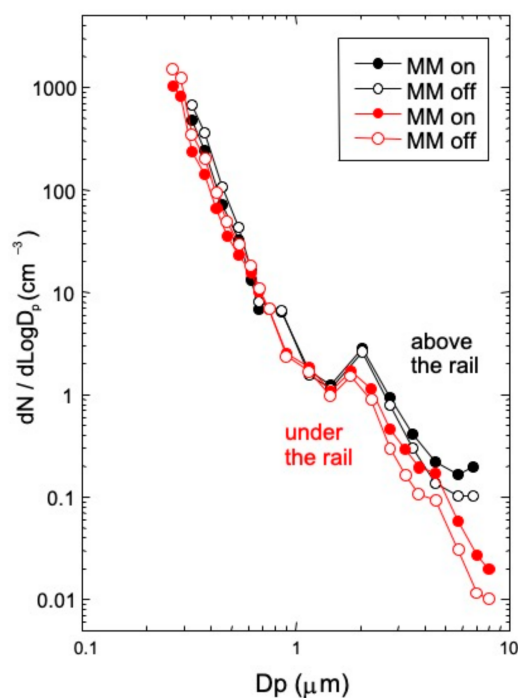


Figure 5. Particle number concentrations (mean values) above (in black) and under the MM rail (in red) at CS during (solid symbols) and out of operation (open symbols) of the MM transport system.

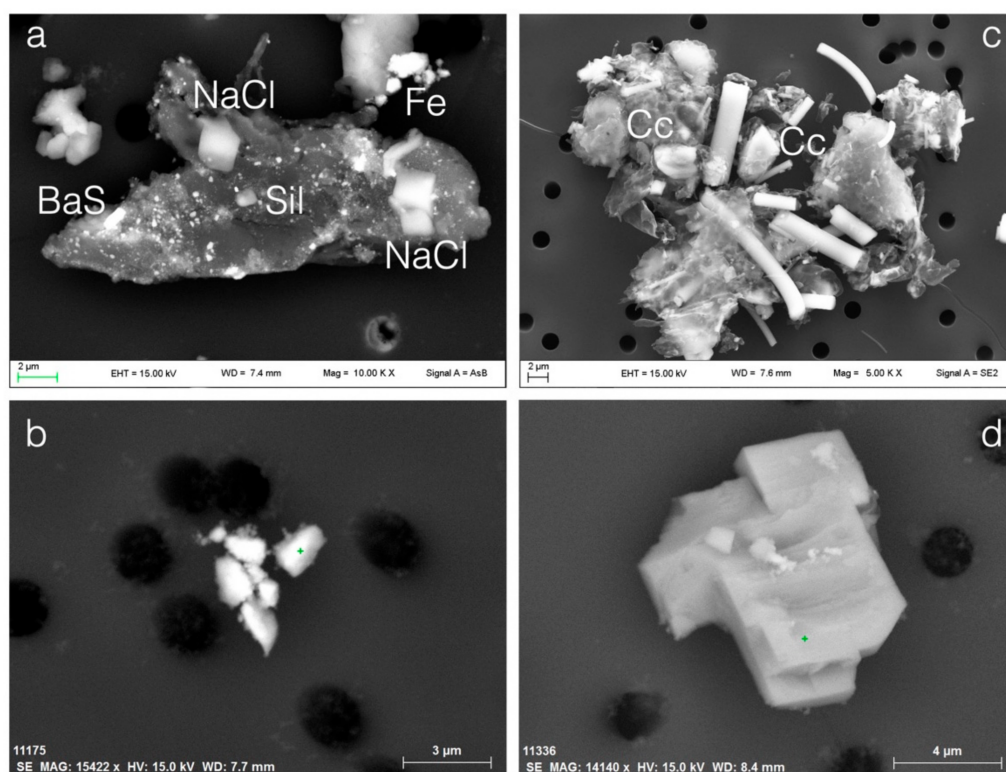


Figure 6. Particle types emitted by MM (SEM micrographs, SE images): (a) rubber fragment with filler inclusions (silicates, Sil; Fe-rich metaloxides, Fe; barium sulfate, BaS) and halite deposits (NaCl), (b) Fe-rich metaloxide individual particles detached from rubber, (c) fiberglass with calcite inclusions (c), and (d) a spatic calcite crystal detached from fiberglass.

The second particle type emitted by MM consist of large fragments of fiberglass (Figure 6c). Calcite crystals are present inside the fiberglass as they are typically used as a filler to improve the mechanical properties of fiberglass (e.g., [37]). It is, thus, very likely that airborne fiberglass fragments result from the wear of the bodywork of the cabins. As in the case of rubber, the fiberglass fragments tend to disintegrate releasing a short number of isolate fibers and numerous calcite particles, both poly-micrometric in size (Figure 6d).

No significant differences were observed between the samples taken in different time slots. At night, in particular, when the MM is not in operation and the cabins are not moving in general, we find the same types of suspended particles. This is in accordance with the particle size distribution (Figure 5) and reveals the occurrence of dust resuspension even in the closing hours of MM.

3.3. Other Sources of PM

In addition to the particles deriving directly from MM, three other particle types have been identified at CS, namely carbonaceous particles, precipitated salts and biogenic particles. Carbonaceous particles are the most abundant among them. They consist of cenospheres and soot. Cenospheres (Figure 7a) have a smooth to rough surface and diameters ranging from 100 to 300 nm. Their composition is dominated by the presence of Si and Al (Table A3). Soot, instead, consist of typical nanoparticle aggregates of variable size, both fresh and, more often, aged (Figure 7b). Cenospheres and soot are more abundant in winter samples, particularly in the sample taken in the afternoon, well in accordance with the observed increase in the concentration of fine particles during the day (Figure 3). In the afternoon samples, in particular, soot is extremely widespread even in the form of small fresh aggregates. Since both particle types are combustion products, the hypothesis is that they come from the outside, i.e., from domestic heating (both types) and from traffic (the former type), and permeate inside the tunnel driven by the air flow of the aeration system. This is in accordance with the trend of the concentration of dust along the tunnel section of MM, which results in decreasing particle number concentrations moving from the tunnel entrance and beyond the CS station. It is quite clear, however, that the ventilation system of MM is not adequate to favor the air exchange inside the tunnel. Rather, it conveys anthropogenic particles from the outside inside the tunnel and, what's more, it keeps the airborne fine particles suspended at any time there inside.

Sodium chloride and alkaline sulfates are the salts identified in our samples. Sodium chloride gives rise to precipitated individual grains cubic or prismatic in shape, or to large, partially dissolved and re-crystallized flower-shaped efflorescences (Figure 7c). Alkaline sulfates, on turn, give rise to rounded or ovoidal single grains or clusters of them (Figure 7d). These precipitates are present in all the samples indicating a great availability of their ionic species in the aerosol at all environmental conditions.

Biogenic particles consist of pollen, spores and fungal conidia (Figure 7e,f). Unlike the others, this particle type was found only in summer, particularly at night. This fact supports the hypothesis of inefficiency of the tunnel's aeration system which seems capable of injecting particles inside rather than conveying them outside while cleaning the air. It is to note, however, that the forced ventilation system is off when the MM line is not in operation.

3.4. Source Profiles and the Impact of MM

Starting from the chemical analyses of PM₁₀ samples, and based on the PM₁₀ values of the sampling site (data provided by the OPC management software), the concentration of different chemical species in the aerosols from CS was calculated for the samples of 12 February and 15 June, which best document the aerosol production by MM in the hours of operation (8 a.m. to 1 p.m., and 3 p.m. to 8 p.m., respectively) in winter and summertime.

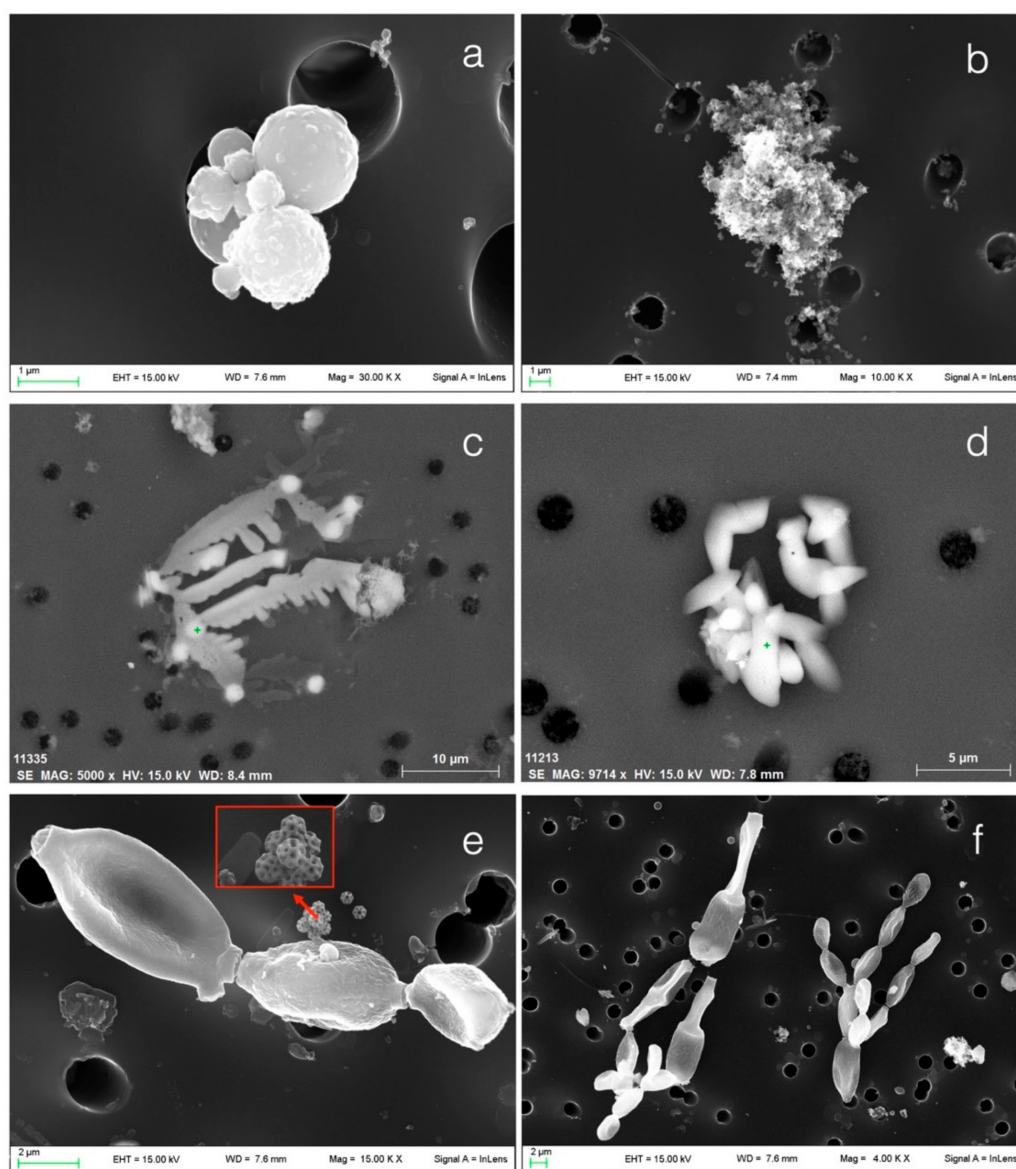


Figure 7. Other particle types (SEM micrographs, SE images): (a) cenospheres, (b) soot, (c) halite, (d) alkali sulfate, (e) pollen and (f) fungal conidia.

The source profiles (Figure 8) are characterized by Si, Al, S, Na and Fe as major elements, and by the minor elements Mg, P and the metals Cr, Mn, Cu and Pb. Based on the results of SEM observations and microanalysis we can assume that most of these elements take part to the rubber composition of the tires and the breaking wheel system (Table A2). The similar trends of Fe, Cr, Mn and Cu in respect to the airborne particulate matter from LRT [38] and metro [39] systems, suggest some influence of mechanical abrasion of the steel rail track too. Al and Si, on turn, are also related to the composition of cenospheres (Table A3; [40]), and this may be the reason for their higher amount in the winter aerosol sample. On the other hand, P and S are also the main components of the biogenic particles (pollen, spores and fungal conidia), and this fact can easily explain the one-order-of-magnitude greater abundance of these chemical species in the summer sample. Na and S, on turn, are also the main components of the salt deposits (chlorides, sulfates; Figure 6a, Figure 7c,d), present in both samples in variable amounts.

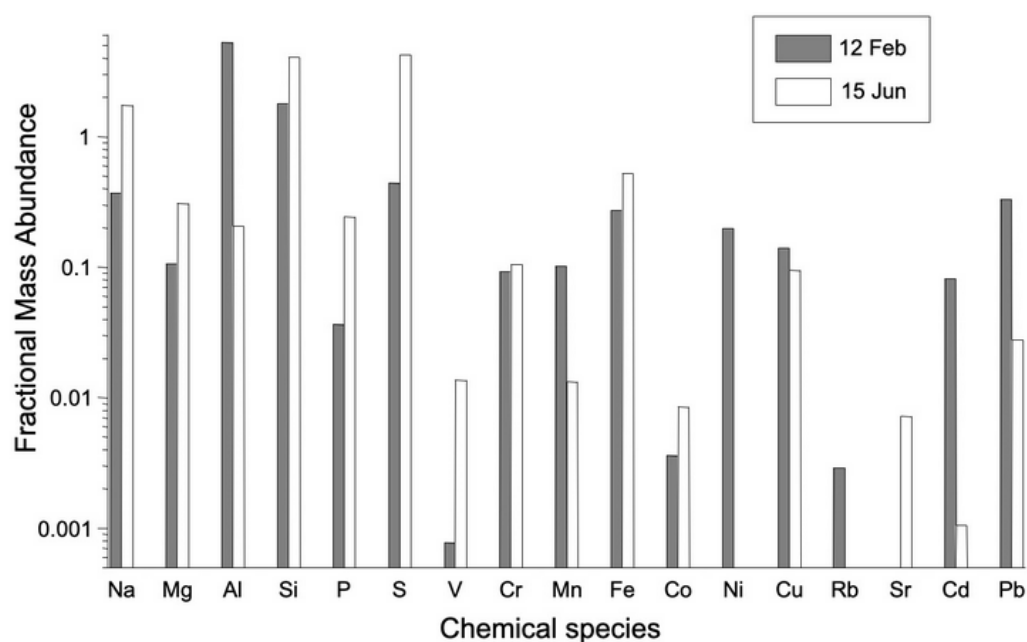


Figure 8. Source profiles of MM road dust emissions at CS in two representative days in winter (12 February) and summertime (15 June).

Lead is, amongst the minor elements and along with cadmium, the only chemical species typically related to vehicular traffic [41–43]. The fact that Pb and Cd are much more abundant in the winter than in the summer sample is a clear evidence of the increased height of the PBL in this latter season, leading to a strong dilution of both these elements in the very bottom of the troposphere. V, Co, Ni, Rb and Sr may be also related to road dust emissions (e.g., [9]).

Additional information on the sources of the different chemical species was obtained by examining the partition of some (other) elements in different particle size ranges (Figure 9). It appears that, of all the analyzed elements, only Ni and Ba are enriched in the fine (and the very fine) fraction of PM₁₀, while all the other elements are variably enriched in the different size classes. Since Ni and Ba are typically related to the production and lifting of road dust (e.g., [44,45]), and since the distribution patterns of these two elements are practically the same at CS and CP, the results demonstrate their common origin from wear of tires and mechanical parts. This means that the particulate sampled at CS comes in part from the outside, and in part is produced by MM. For the same reasons, the analogous distribution patterns of Al, Cr and Mn at CS and CP support the same origin and mode of dispersion of particulate matter in the two sites. Regarding Al, in particular, it is not possible to exclude its origin also from natural dust sources, be it local or transported, as already hypothesized in the case of the summer sample. However, the fact that the Al contents are, on the same day, higher at CS rather than CP contrasts with a natural origin of dust while it is perfectly consistent with the broader hypothesis of a contribution from road dust.

Fe, Pb and, in some respects, Cu show different distributions at CP and CS. At CP Fe and Cu show a bimodal trend of enrichment while Pb is enriched in the fine fraction. At CS, instead, Fe is distributed in all classes with a slight prevalence in the fine fraction while Cu and Pb concentrate in the coarse fraction. Pb, in particular, is 7–10 times enriched in the >4.2 μm than in the fine size range, and even almost 100 times more abundant than it is, in the same class at CP.

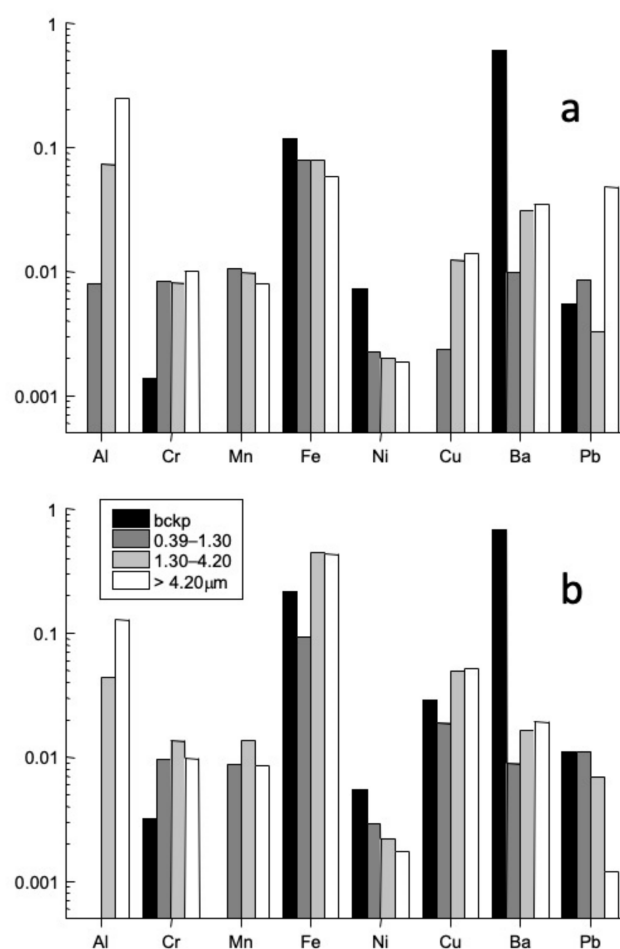


Figure 9. Source profiles of winter samples from CS (a) and CP (b) in different particle size ranges.

We know from SEM observations at CS that Fe and Cu are typically related to MM emissions (mainly rubber fragments; see Section 3.2) and, indeed, they are enriched in those fractions. In light of this, the bimodal patterns of the same two elements at CP denote the presence of a second dust component in respect to MM, either natural (in the case of Fe) and/or anthropic (road dust; in the case of Cu) at CP. The trend of Pb at CP supports the occurrence of this last component, anthropogenic in origin, in the outside. Therefore, the strong enrichment in Pb of the large coarse fraction at CS can be explained by the entry of Pb from the outside as a direct emission of vehicular traffic, and by its subsequent adhesion to the coarse particulate produced there by MM. We can thus conclude that the basic similarity between the two sites be linked to the wear of tires and/or mechanical parts in both urban contexts. These results highlight the remarkable contribution of road dust in the center of Perugia, meaning road dust both the one produced and raised by urban traffic, and the one emitted by MM during operation.

3.5. Carbonaceous Aerosol and the Impact of Combustive Sources

Carbonaceous particles are, after the road dust, the second type of particles found in our samples. To understand its relevance in urban aerosol in Perugia we examined its trend and values in the three different monitoring sites during the intensive campaigns. The graphs in Figure 10 show the trend of the concentration in air of NPs and BC measured, in the same time interval and in dynamic conditions, on 10 February and 16 June 2015. In the graphs, the colored lines represent the passages of the cabin in the sites of interest (CS, CP, CR).

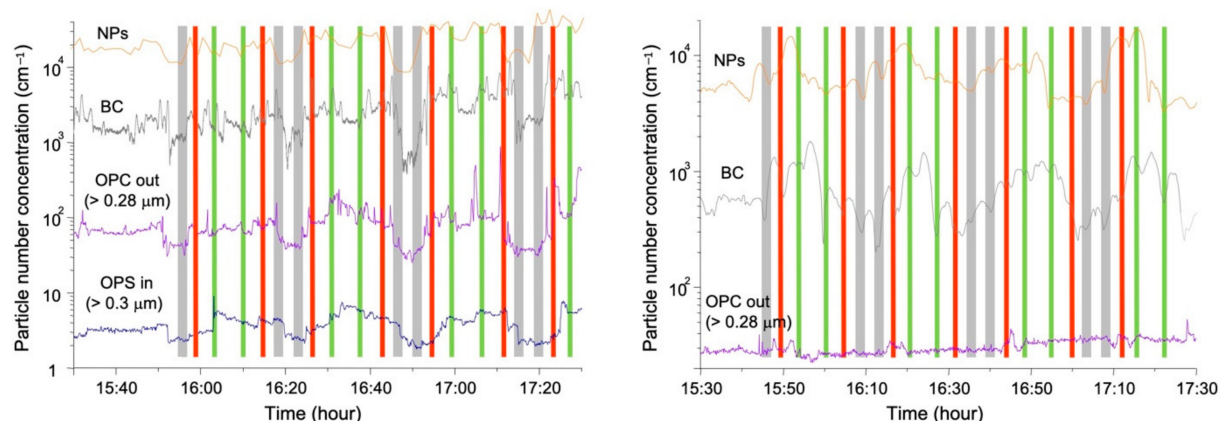


Figure 10. Trends of particle number concentration of finest particles, nanoparticles (NPs) and black carbon (BC) from dynamic measurements performed at CS (grey), CR (red) and CP (green) on 10 February (**left** panel) and 16 June 2015 (**right** panel). In February measurements were performed both outside (OPC out) and inside (OPS in) the cabin. This is the reason for the particle size ranges provided by the counters are different.

Our main observation is the general correspondence of the trends of BC and NPs. This correspondence is very good in winter for the high signal-to-noise ratios, and much weaker in summer due to the five times lower concentrations in this latter period. When looking in more detail, however, some mismatch between BC and NPs trends does, actually, exist in both cases, though it is particularly evident in summertime since the lowest concentrations increase the amplitude of fluctuations. Such a mismatch reveals the presence of fine BC particles, and the presence of non-BC NPs in the aerosols. While the fine BC particles possibly consist of fresh or, more likely, aged soot, the nature of non-BC NPs is much more uncertain. Looking at the chemical data (Figure 9) we can assume that they are metal- (e.g., Fe and/or Ni) or alkali metal- (e.g., Ba) bearing NPs from the road dust.

In winter, the trend of NPs essentially follows that of the smallest fine particles detected by optical particle counters. The much lower values of the concentrations and the slight delay of the measurements inside compared to those outside the cabin are also noteworthy. This suggests some kind of a shielding action by the cabins against pollutants present outside, along with the maintenance of the pollutant concentrations at the MM stations (where the doors are open to allow passengers boarding and descent) inside the cabins of the MM line.

CS does generally show the lowest BC values. Regarding the other two sites, and contrary to expectations, BC concentrations are not always higher at CR (crossroad) than at CP (urban background). Such a discrepancy has no simple explanation considering the higher amount of traffic emissions (e.g., NO) at CR in respect to CP [28]. It may depend on local dilution of the particulate pollutants due to (micro)environmental conditions.

In order to evaluate the incidence of BC within the carbonaceous particulate matter, we considered the concentrations of elemental carbon (EC) and organic carbon (OC) in our PM_{2.5} samples at CS. We know in fact that BC and EC are products of combustion, and that they do generally coincide in soot. We also know that OC can be of primary origin (i.e., combustion of biomass and fossil fuels, or biogenic; [46]) or secondary origin (VOCs oxidation; [47]). In our case we must also consider rubber as a primary source of OC. The OC and EC aerosol concentrations at CS at different times in the two periods of interest are shown in Table 2. The OC values are 2–3 times lower, as well as much more stable, in summer than in winter, likely due to a substantial biogenic contribution compared to the contribution of combustion in that period. The conspicuous presence of pollen and spores in summer, and the variable abundance of cenospheres in winter, support this hypothesis. The EC values, on turn, range from a minimum of 0.25 $\mu\text{g m}^{-3}$ to a maximum of 2.20 $\mu\text{g m}^{-3}$, they are lower at night and higher during traffic rush hours, well in accordance with the conspicuous presence of soot found in these samples (see

Section 3.3). The EC values and the values of the OC/EC ratio in our samples are consistent with those of urban background at peak traffic hours in the case of the higher EC values, and with rural environments in the other cases [33].

In conclusion, our data reveal BC as a main part in the nanoparticle component of PM₁₀ in Perugia, and that this component is equally or even less relevant than the biogenic and combustion component of biomass in the composition of the carbonaceous particulate matter.

Table 2. OC and EC concentrations ($\mu\text{g m}^{-3}$) in PM_{2.5} at CS and corresponding values of the OC/EC ratio.

Date	Time	OC	EC	OC/EC
10 February 2015	3 p.m.–8 p.m.	8.09	0.92	8.8
12 February 2015	0 a.m.–5 a.m.	5.48	0.79	6.9
13 February 2015	8 a.m.–1 p.m.	11.92	2.20	5.4
16 June 2015	3 p.m.–8 p.m.	3.30	1.04	3.2
18 June 2015	0 a.m.–5 a.m.	3.00	0.25	12
19 June 2015	8 a.m.–1 p.m.	3.38	1.54	2.2

3.6. Road Dust and Air Quality in Perugia

We have seen that road dust and carbonaceous particles are two types of particles well represented in the urban aerosol of Perugia, and that MM is an independent and remarkable source of road dust. Based on the observations and considerations made in the previous sections, we thus attempted an estimate of the incidence of road dust in the urban aerosol of Perugia.

To do this we took under consideration the OC and EC concentrations in our CS samples. We know that the OC values provide an excess estimate of the organic component of rubber considering the additional contribution of biomass combustion in winter and of the biogenic component in summer. For these reasons, and in order to simplify, we considered the average OC concentration in summer, equal to $3.2 \mu\text{g m}^{-3}$, to represent the mean rubber contribution to OC. Based on the stationary and dynamic measurements at CS, providing a PM₁₀ concentration of $16 \mu\text{g m}^{-3}$ in the days of interest, we obtain a quantitative estimate of the fraction of road dust in the PM₁₀ at CS equal to 20 wt%. In the case of soot, for which we assumed a concentration of EC equal to the average of the values obtained in the six different samples analyzed ($1.12 \mu\text{g m}^{-3}$), we obtained a mass fraction of carbonaceous particulate within the PM₁₀ of 7 wt%. These values do, actually, provide a rough estimate of the contribution of road dust to the urban aerosol of Perugia since the OC and EC values refer to PM_{2.5} instead of PM₁₀.

After having estimated the extent of MM emissions, we were able to estimate the contribution of MM in the urban aerosol of Perugia. In 2015, the year in which the intensive campaigns were carried out, the values of the fraction of MM and soot in PM₁₀ that we obtained were equal to 11 wt% and 4 wt%, respectively, for an average concentration of PM₁₀ in Perugia of $28 \mu\text{g m}^{-3}$. Similar values were found for the subsequent five-year period in which the average concentration of PM₁₀ was equal to $23 \mu\text{g m}^{-3}$, which provides a mean value of the fraction of road dust emitted by MM equal to 14 wt%.

The value obtained is remarkably similar to the value resulting from PMF source apportionment of PM₁₀ aerosol samples collected at CP during a one-year sampling campaign [24]. It can, thus, be considered a reliable estimate of the MM contribution to the road dust in Perugia. The values are also consistent with those reported for other, though different, urban contexts in Europe [9,48,49]. In any case the obtained estimate is to be considered in defect since it is based on quantitative determinations of the OC fraction on PM_{2.5}. In addition, we have to consider that the particulate emitted by MM is not made only of rubber, but also contains filler particles of different size capable, as evidenced by SEM results, of being detached from the rubber during its degradation. Furthermore, we have to consider the presence, on the outside, of road dust s.s. due to traffic. The

contribution of this latter component, though similar to that of MM for many elements and constant throughout the year, adds to that of MM.

In the light of all these points, and despite the substantially coarse dimensions of the particulate matter emitted by MM, such as to make it respirable only in part, the contribution of MM to the aerosol in Perugia cannot be neglected, both in absolute terms and in relation to the contribution of combustive sources related to traffic. Considering the pollutant concentrations and the time of stationing of the public in the MM transport system, the dose that we must expect in relation to exposure is not high. However, we cannot forget that MM adds road dust to the road dust already present in the outside as a result of traffic. The effects of this exposure, as widely observed also in the literature [50–52], are not foreseeable at the moment nor they have been systematically studied. For this reason, and because of the variable and distinctive physico-chemical characteristics of the emitted particulate, such kind of emissions have to be monitored in detail.

4. Concluding Remarks

In this paper the nature and consistency of the sources of particulate matter in the city center of Perugia have been investigated, with special regard to the MM local LRT system. To this aim, a two-week intensive sampling and measurement campaign was conceived in the context of a three-year long monitoring campaign. The results of the present study were compared with the results of the statistical analysis of the whole campaign in order to extrapolate the “physical” meaning of the processes.

Despite its short duration, the intensive campaign revealed the essence of the processes and allowed an estimate of the impact of MM as a source of particulate matter in the urban aerosol of Perugia. In particular, the results show that MM is a considerable source of atmospheric particulate matter, and that this particulate has characteristics very similar to those of common urban road dust in Perugia. We can thus expect that, due to the abundance and variety of components, these two types of dust can act both individually and synergistically in modulating the properties and effects of urban aerosol in Perugia.

Passengers are exposed to the road dust particulate pollutants both indoors (i.e., in the tunnel and at CS) and outdoors (i.e., along the route). Indoors, this is also partly due to the inadequacy of the tunnel ventilation system, which lets the PM enter from the outside and, at the same time, keeps the particulate suspended. Outdoors this is due to the fact that the cabins pass through areas with different pollutant types which, indeed, permeate the interior of the cabins in variable extent. We can assume that the average exposure is low due to the low values of concentrations we have estimated, and the short exposure times. However, no clear indications are provided on the effects of road dust and the way to mitigate them for the lack of epidemiological studies on this topic. This is just the reason to pay increasing attention to the environmental monitoring of road dust and its possible effects by means of more careful and targeted studies. The results of this study, thus, pave the way for targeted, multidisciplinary toxicological and epidemiological studies on the dose effect of MM in Perugia, and of road dust in general.

Author Contributions: Conceptualization, B.M.; methodology, B.M.; software, S.C.; validation, S.C. and B.M.; aerosol sampling and measurements, B.M., C.P., A.D.M.d.B., G.C. and L.F.; chemical analysis, F.B. and D.C.; investigation, B.M. and S.C.; data curation, B.M. and S.C.; writing—original draft preparation, B.M.; writing—review and editing, B.M., S.C. and D.C.; funding acquisition, D.C. All authors have read and agreed to the published version of the manuscript.

Funding: This research received no external funding.

Institutional Review Board Statement: Not applicable.

Informed Consent Statement: Not applicable.

Data Availability Statement: The data presented in this study are available on request from the corresponding author.

Acknowledgments: The authors thank ARPA Umbria and the municipality of Perugia for having supported and favored the measurement and analysis activities in the context of a dedicated project (PMetro project). In particular, the authors sincerely thank the analysts A. Pileri and M. Galletti, both from ARPA Umbria, who carried out the EC/OC analyses on CS and CP winter samples. The authors also wish to thank FAI Instruments, for helping in the customization and setting of the the OPC used in the cabin. Thanks to the staff of Leitner, manufacturer and coordinator of the maintenance of the ropeway system employed in MM, and in particular P. Vinatzer (head technician) for the constant support during all the activities carried out. We thank MIUR and University of Perugia for financial support through AMIS project (“Dipartimenti di Eccellenza–2018–2022”). We also acknowledge the GEMMA center in the framework of the MIUR project “Dipartimenti di Eccellenza 2018–2022”.

Conflicts of Interest: The authors declare no conflict of interest.

Appendix A. Details of Sampling and Measurement Procedures

The intensive campaigns involved a series of instruments and procedures for collecting data and samples Table A1 reports the complete arrangement of the instruments employed, their location and the period of use during the intensive campaigns.

Table A1. Measurement and sampling layout.

		Instrumentation	Where	When	Time
Measurements	stationary	OPC (GRIMM)	CS	9–13 Feb	H 24
		OPS (TSI)	CS	15–19 Jun	H 24
		CPC	CS, CP	9–13 Feb 15–19 Jun	0 a.m.–2 a.m. 8 a.m.–10 a.m. 4 p.m.–6 p.m.
	dynamic	OPC (FAI)	Cabin-out	9–13 Feb 15–19 Jun	6 a.m.–9 p.m.
		OPS (TSI)	Cabin-in	10 Feb 16 Jun	3 p.m.–6 p.m.
		μ -aethalometer miniDiSC	Cabin-out	10 Feb 16 Jun	3 p.m.–6 p.m.
Sampling	ECHO-PM	CS	9 Feb (PM ₁₀)	3 p.m.–8 p.m.	
			10 Feb (PM _{2.5})	3 p.m.–8 p.m.	
			11 Feb (PM ₁₀)	0 a.m.–5 a.m.	
			12 Feb (PM _{2.5})	0 a.m.–5 a.m.	
			12 Feb (PM ₁₀)	8 a.m.–1 p.m.	
			13 Feb (PM _{2.5})	8 a.m.–1 p.m.	
			15 Jun (PM ₁₀)	3 p.m.–8 p.m.	
			16 Jun (PM _{2.5})	3 p.m.–8 p.m.	
			17 Jun (PM ₁₀)	0 a.m.–5 a.m.	
			18 Jun (PM _{2.5})	0 a.m.–5 a.m.	
			18 Jun (PM ₁₀)	8 a.m.–1 p.m.	
19 Jun (PM _{2.5})	8 a.m.–1 p.m.				

Appendix B. Preliminary Campaign

A preliminary measurement and sampling campaign was carried out from 21 to 25 January 2013. The campaign involved stationary measurements performed in the whole period using two distinct optical particle counters working in pair, namely the OPS positioned at the side of the MM track, at eye level, and the GRIMM positioned below the rails.

Sampling took place from 22 to 24 January 2013. Two high-volume aerosol samplers (HVS, TISCH TE6001, 1140 L min⁻¹) working in pair continuously were employed at CS and CP. The instruments were operated with PM₁₀ impactor and three size stages (0.39, 1.3 and 4.2 μ m cut-off) plus backup on 203 × 254 mm quartz fiber filters (Whatman QM-A).

The samples were analysed in the laboratory of ARPA Umbria by Atomic Absorption Spectrometry (AANALYST 600, Perkin-Elmer, Waltham MA, USA). The analyses were

performed Small fragment (2×2 cm) of the filters were cut using ceramic scissors Part of the filters are digested with 8 mL concentrated nitric acid HNO_3 (Trace select[®] for trace analysis, Fluka Sigma-Aldrich, St. Louis, MO, USA) and 2 mL of hydrogen peroxide H_2O_2 (Trace Select[®] Ultra $\geq 30\%$, Fluka Sigma-Aldrich) in a micro-wave digestion system (Start E, Milestone, Shelton, CT, USA). The acid solutions diluted with ultrapure-MilliQ water, were analyzed by Atomic Absorption Spectrometer (AANALYST 600, Perkin-Elmer).

Appendix C. Individual Particle SEM-EDS Mapping and Microanalysis

Representative mapping and analyses are reported in Figure A1 and Tables A2 and A3, respectively.

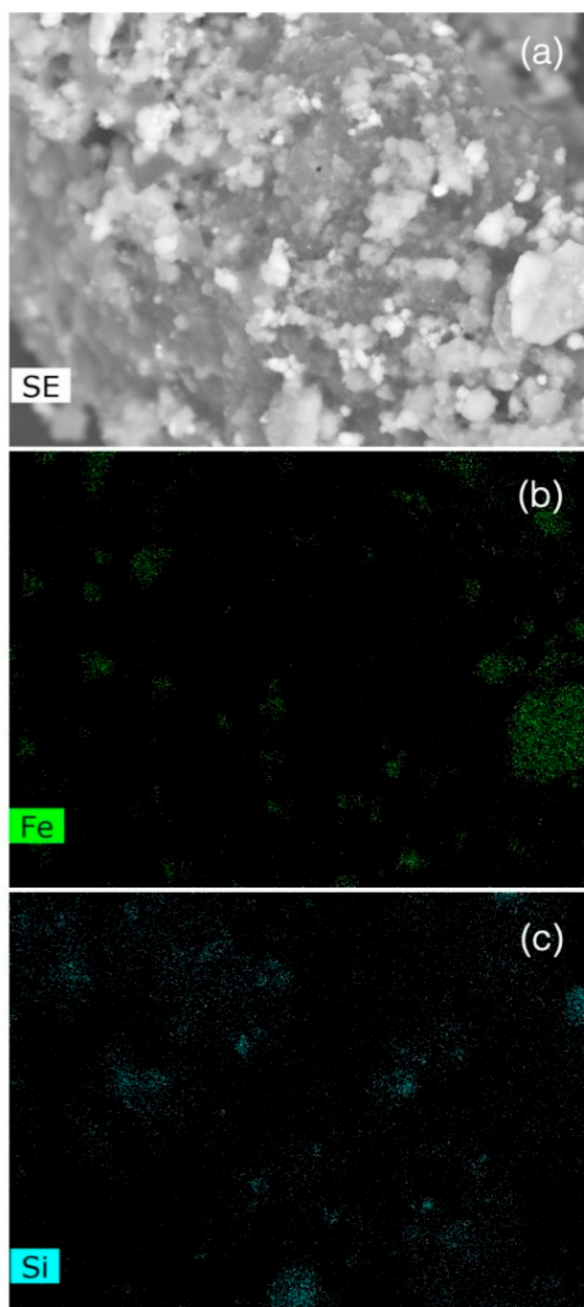


Figure A1. SEM micrograph of the surface of a rubber particle (a) with corresponding EDS element distribution maps of iron (b) and silicon (c).

Table A2. Representative SEM-EDS bulk chemical analyses * of rubber particles.

Element (wt%)	# 1	# 2	# 3	# 4
Oxygen	53.99	48.46	51.58	59.06
Aluminium	8.20	0.07	13.97	6.03
Silicon	17.20	0.13	19.76	11.44
Calcium	2.28	-	0.51	2.02
Potassium	3.30	-	8.04	3.86
Magnesium	1.58	-	1.75	0.77
Chlorine	1.71	2.57	0.08	1.52
Iron	6.40	33.54	3.33	11.74
Zinc	4.36	14.33	-	1.47
Sulfur	0.12	0.34	0.05	0.56
Titanium	0.11	-	0.06	-
Copper	0.73	0.55	0.49	-
Sodium	-	-	0.35	0.62
Barium	-	-	-	0.82
Phosphorus	-	-	-	0.04

* Carbon has been removed from analyses due to its use for conductive coating of the samples.

Table A3. Representative SEM-EDS chemical analyses * of cenospheres.

Element (wt%)	# 1	# 2	# 3	# 4	# 5
Oxygen	54.48	66.51	62.52	56.28	62.96
Iron	8.59	4.31	5.98	5.62	4.23
Aluminum	10.09	10.60	11.35	13.61	8.89
Silicon	17.61	13.65	14.32	17.19	11.94
Potassium	1.39	0.66	0.96	0.88	0.20
Calcium	2.33	0.37	2.09	2.57	6.93
Titanium	1.57	-	0.57	0.87	0.20
Sodium	0.66	2.02	0.58	0.80	0.42
Magnesium	1.15	0.66	1.53	1.64	2.01
Sulfur	0.10	-	0.02	0.29	1.04
Barium	-	1.20	-	-	-
Phosphorous	-	-	0.06	0.22	1.55

* Carbon has been removed from analyses due to its use for conductive coating of the samples.

References

- Ham, W.; Vijayan, A.; Schulte, N.; Herner, J.D. Commuter exposure to PM_{2.5}, BC, and UFP in six common transport microenvironments in Sacramento, California. *Atmos. Environ.* **2017**, *167*, 335–345. [[CrossRef](#)]
- Fruin, S.; Westerdahl, D.; Sax, T.; Sioutas, C.; Fine, P.M. Measurements and predictors of on-road ultrafine particle concentrations and associated pollutants in Los Angeles. *Atmos. Environ.* **2008**, *42*, 207–219. [[CrossRef](#)]
- Weber, S. Spatio-temporal covariation of urban particle number concentration and ambient noise. *Atmos. Environ.* **2009**, *43*, 5518–5525. [[CrossRef](#)]
- Shu, S.; Yang, P.; Zhu, Y. Correlation of noise levels and particulate matter concentrations near two major freeways in Los Angeles, California. *Environ. Pollut.* **2014**, *193*, 130–137. [[CrossRef](#)] [[PubMed](#)]
- Delfino, R.J. Epidemiologic evidence for asthma and exposure to air toxics: Linkages between occupational, indoor, and community air pollution research. *Environ. Health Perspect.* **2002**, *110*, 573–589. [[CrossRef](#)] [[PubMed](#)]
- Lipofert, F.W.; Wyzga, R.E. On exposure and response relationships for health effects associated with exposure to vehicular traffic. *J. Expo. Sci. Environ. Epidemiol.* **2008**, *18*, 588–599. [[CrossRef](#)]
- Camusso, C.; Pronello, C. A study of relationships between traffic noise and annoyance for different urban site typologies. *Transp. Res. Part D Transp. Environ.* **2016**, *44*, 122–133. [[CrossRef](#)]
- Sabbir Ahmed, C.M.; Jiang, H.; Chen, J.Y.; Lin, Y.-H. Traffic-related particulate matter and cardiometabolic syndrome: A review. *Atmosphere* **2018**, *9*, 336. [[CrossRef](#)]
- Amato, F.; Cassee, F.R.; Denier van der Gon, H.A.C.; Gehrig, R.; Gustafsson, M.; Hafner, W.; Harrison, R.M.; Jozwicka, M.; Kelly, F.J.; Moreno, T.; et al. Urban air quality: The challenge of traffic non-exhaust emissions. *J. Hazard. Mater.* **2014**, *275*, 31–36. [[CrossRef](#)]

10. Perrone, M.G.; Larsen, B.R.; Ferrero, L.; Sangiorgi, G.; De Gennaro, G.; Udisti, R.; Zangrando, R.; Gambaro, A.; Bolzacchini, E. Sources of high PM_{2.5} concentrations in Milan, Northern Italy: Molecular marker data and CMB modelling. *Sci. Total Environ.* **2012**, *414*, 343–355. [[CrossRef](#)]
11. Sindhwani, R.; Goyal, P. Assessment of traffic-generated gaseous and particulate matter emissions and trends over Delhi (2000–2010). *Atmos. Pollut. Res.* **2014**, *5*, 438–446. [[CrossRef](#)]
12. Ferrero, L.; Cappelletti, D.; Moroni, B.; Sangiorgi, G.; Perrone, M.G.; Crocchianti, S.; Bolzacchini, E. Wintertime aerosol dynamics and chemical composition across the mixing layer over basin valleys. *Atmos. Environ.* **2012**, *56*, 143–153. [[CrossRef](#)]
13. Moroni, B.; Cappelletti, D.; Marmottini, F.; Scardazza, F.; Ferrero, L.; Bolzacchini, E. Integrated single particle-bulk chemical approach in the characterization of local and long range sources of particulate pollutants. *Atmos. Environ.* **2012**, *50*, 267–277. [[CrossRef](#)]
14. Stavroulas, I.; Bougiatioti, A.; Grivas, G.; Paraskevopoulou, D.; Tsagkaraki, M.; Zarmas, P.; Liakakou, E.; Gerasopoulos, E.; Mihalopoulos, N. Sources and processes that control the submicron organic aerosol composition in an urban Mediterranean environment (Athens): A high temporal-resolution chemical composition measurement study. *Atmos. Chem. Phys.* **2019**, *19*, 901–919. [[CrossRef](#)]
15. Moreno, T.; Pérez, N.; Reche, C.; Martins, V.; de Miguel, E.; Capdevila, M.; Centelles, S.; Mingillon, M.C.; Amato, F.; Alastuey, A.; et al. Subway platform air quality: Assessing the influences of tunnel ventilation, train piston effect and station design. *Atmos. Environ.* **2014**, *92*, 461–468. [[CrossRef](#)]
16. Karagulian, F.; Belis, C.A.; Dora, C.F.C.; Prüss-Ustün, A.M.; Bonjour, S.; Adair-Rohani, H.; Amann, M. Contributions to cities' ambient particulate matter (PM): A systematic review of local source contributions at global level. *Atmos. Environ.* **2015**, *120*, 475–483. [[CrossRef](#)]
17. Buhrmann, S.; Wefering, F.; Rupperecht, S. *Guidelines for Developing and Implementing a Sustainable Urban Mobility Plan*, 2nd ed.; Rupperecht Consult-Forschung und Beratung GmbH: Köln, Germany; Available online: https://www.eltis.org/sites/default/files/guidelines_for_developing_and_implementing_a_sustainable_urban_mobility_plan_2nd_edition.pdf (accessed on 28 August 2021).
18. EU. *Directive (EU) 2016/2284 of the European Parliament and of the Council of 14 December 2016 on the Reduction of National Emissions of Certain Atmospheric Pollutants*; EU: Brussels, Belgium, 2016.
19. Pisoni, E.; Christidis, P.; Thunis, P.; Trombetti, M. Evaluating the impact of “Sustainable Urban Mobility Plans” on urban background air quality. *J. Environ. Manag.* **2019**, *231*, 249–255. [[CrossRef](#)] [[PubMed](#)]
20. Garcia, H.M.; de la Calle, V.M.; Claudia, Y. Cultural heritage and urban tourism: Historic city centres under pressure. *Sustainability* **2017**, *9*, 1346. [[CrossRef](#)]
21. Wang, Q.; Sun, H. Traffic Structure Optimization in historic districts based on green transportation and sustainable development concept. *Adv. Civ. Eng.* **2019**. [[CrossRef](#)]
22. Park, E.S.; Sener, I.N. Traffic-related air emissions in Houston: Effects of light-rail transit. *Sci. Total Environ.* **2019**, *651*, 154–161. [[CrossRef](#)]
23. Houston, D.; Dang, A.; Wu, J.; Chowdhury, Z.; Edwards, R. The cost of convenience; air pollution and noise on freeway and arterial light rail station platforms in Los Angeles. *Transp. Res. Part D Transp. Environ.* **2016**, *49*, 127–137. [[CrossRef](#)]
24. Cappelletti, D.; Castellini, S.; Moroni, B.; Scardazza, F. Caratteristiche Morfologiche e Chimiche Delle Polveri Fini in Umbria. Dati. 2013. Available online: <https://www.arpa.umbria.it/resources/docs/relazione-polveri-pg-2013.pdf> (accessed on 7 October 2021).
25. Hoffmann, K.; Liehl, R. Cable-drawn urban transport systems. In *Urban Transport XI. WIT Transactions on the Built Environment*; Brebbia, C.A., Ed.; WIT Press: Southampton, UK, 2005; Volume 77, pp. 25–36.
26. Castellini, S.; Moroni, B.; Cappelletti, D. PMetro: Measurement of urban aerosols on a mobile platform. *Measurement* **2014**, *49*, 99–106. [[CrossRef](#)]
27. Moroni, B.; Castellini, S.; Crocchianti, S.; Cappelletti, D.; Ferrero, L.; Salvatori, R.; Ianniello, A.; Spataro, F.; Esposito, G. Sources, fate and dynamics of dispersion of aerosol particles in historic cities: The case of Perugia (Central Italy). In *Proceedings of the DUST2014, Castellaneta Marina, Italy, 1–6 June 2014*. [[CrossRef](#)]
28. Del Sarto, S.; Ranalli, M.G.; Cappelletti, D.; Moroni, B.; Crocchianti, S.; Castellini, S. Modeling spatio-temporal air pollution data from a mobile monitoring station. *J. Stat. Comput Simul.* **2016**. [[CrossRef](#)]
29. Crocchianti, S.; Del Sarto, S.; Ranalli, M.G.; Moroni, B.; Castellini, S.; Petroselli, C.; Cappelletti, D. Spatiotemporal correlation of urban pollutants by long-term measurements on a mobile observation platform. *Environ. Pollut.* **2021**, *268*. [[CrossRef](#)] [[PubMed](#)]
30. Fierz, M.; Houle, C.; Steigmeier, P.; Burtscher, H. Design, Calibration, and Field Performance of a Miniature Diffusion Size Classifier. *Aerosol Sci. Tech.* **2011**, *45*, 1–10. [[CrossRef](#)]
31. Vecchi, R.; Piziali, F.A.; Favaron, M.; Bernardoni, V. Radon-based estimates of equivalent mixing layer heights: A long-term assessment. *Atmos. Environ.* **2019**, *197*, 150–158. [[CrossRef](#)]
32. Castellini, S.; Moroni, B.; Ranalli, M.G.; Lama, G.; Eheim, M.; Ferrera, R.; Trapani, A.; Cappelletti, D. Real time monitoring of urban particulate matter on a mobile platform. In *Proceedings of the 4th Imeko TC19 Symposium on Environmental Instrumentation and Measurements, Lecce, Italy, 3–4 June 2013*; pp. 5–8, ISBN 9788896515204.
33. Sandrini, S.; Fuzzi, S.; Piazzalunga, A.; Prati, P.; Bonasoni, P.; Cavalli, F.; Bove, M.C.; Calvello, M.; Cappelletti, D.; Colombi, C.; et al. Spatial and seasonal variability of carbonaceous aerosol across Italy. *Atmos. Environ.* **2014**, *99*, 587–598. [[CrossRef](#)]

34. Baranek, T.M. High density metaloxide fillers in rubber compounds. US Patent 6,734,245 B2, 11 May 2004.
35. Hanafi, I.; Hakimah, O.; Azlan, A. The Effect of Feldspar Loading on Curing Characteristics, Mechanical Properties, Swelling Behavior and Morphology of Natural Rubber Vulcanizates. *Int. J. Polym. Mater.* **2005**, *54*, 43–62. [[CrossRef](#)]
36. Shahzamani, M.; Rezaeian, I.; Loghmani, M.S.; Zahedi, P.; Rezaeian, A. Effects of BaSO₄, CaCO₃, kaolin and quartz fillers on mechanical, chemical and morphological properties of cast polyurethane. *Plast. Rubber Compos.* **2012**, *41*, 263–269. [[CrossRef](#)]
37. Rothon, R.; Paynter, C. Calcium Carbonate Fillers. In *Fillers for Polymer Applications. Polymers and Polymeric Composites: A Reference Series*; Rothon, R., Ed.; Springer: Cham, Switzerland, 2017. [[CrossRef](#)]
38. Cartledge, B.T.; Majestic, B.J. Metal concentrations and soluble iron speciation in fine particulate matter from light rail activity in the Denver-Metropolitan area. *Atmos. Pollut. Res.* **2015**, *6*, 495–502. [[CrossRef](#)]
39. Querol, X.; Moreno, T.; Karanasiou, A.; Reche, C.; Alastuey, A.; Viana, M.; Font, O.; Gil, J.; de Miguel, E.; Capdevila, M. Variability of levels and composition of PM₁₀ and PM_{2.5} in the Barcelona metro system. *Atmos. Chem. Phys.* **2012**, *12*, 5055–5076. [[CrossRef](#)]
40. Ranjba, N.; Kuenze, C. Cenospheres: A review. *Fuel* **2017**, *207*, 1–12. [[CrossRef](#)]
41. Gunawardana, C.; Goonetilleke, A.; Egodawatta, P.; Dawes, L.; Kokot, S. Source characterisation of road dust based on chemical and mineralogical composition. *Chemosphere* **2012**, *2*, 163–170. [[CrossRef](#)]
42. Wang, G.; Wu, Y.; Lin, Y. Trace element analysis of extraterrestrial metal samples by inductively coupled plasma mass spectrometry: The standard solutions and digesting acids. *Rapid Commun. Mass Spectrom.* **2016**, *30*, 543–551. [[CrossRef](#)]
43. Szwalec, A.; Mundala, P.; Kedzior, R.; Pawlik, J. Monitoring and assessment of cadmium, lead, zinc and copper concentrations in arable roadside soils in terms of different traffic conditions. *Environ. Monit. Assess.* **2020**, *192*, 155. [[CrossRef](#)]
44. Adamiec, E.; Jarosz-Krzeminska, E.; Wieszala, R. Heavy metals from non-exhaust vehicle emissions in urban and motorway road dusts. *Environ. Monit. Assess.* **2016**, *188*, 369. [[CrossRef](#)] [[PubMed](#)]
45. Miazgowicz, A.; Kremmhuber, K.; Lanzerstorfer, C. Metals concentrations in road dust from high traffic and low traffic area: A size dependent comparison. *Int. J. Environ. Sci. Technol.* **2020**, *17*, 3365–3372. [[CrossRef](#)]
46. Briggs, N.L.; Long, C.M. Critical review of black carbon and elemental carbon source apportionment in Europe and the United States. *Atmos. Environ.* **2016**, *144*, 409–427. [[CrossRef](#)]
47. Mayorga, R.J.; Zhao, Z.; Zhang, H. Formation of secondary organic aerosol from nitrate radical oxidation of phenolic VOCs: Implications for nitration mechanisms and brown carbon formation. *Atmos. Environ.* **2020**. [[CrossRef](#)]
48. Amato, F.; Pandolfi, M.; Moreno, T.; Furger, M.; Pey, J.; Alastuey, A.; Bukowiecki, N.; Prevot, A.S.H.; Baltensperger, U.; Querol, X. Sources and variability of inhalable road dust particles in three European cities. *Atmos. Environ.* **2011**, *45*, 6777–6787. [[CrossRef](#)]
49. Amato, F.; Favez, O.; Pandolfi, M.; Alastuey, A.; Querol, X.; Moukhtar, S.; Bruge, B.; Verlhac, S.; Orza, J.A.G.; Bonnaire, N.; et al. Traffic induced particle resuspension in Paris: Emission Factors and source contributions. *Atmos. Environ.* **2016**, *129*, 114–124. [[CrossRef](#)]
50. Khan, R.K.; Strand, M.A. Road dust and its effect on human health: A literature review. *Epidemiol. Health* **2018**, *40*, e2018013. [[CrossRef](#)]
51. Candeias, C.; Vicente, E.; Tomé, M.; Rocha, F.; Avila, P.; Célia, A. Geochemical, mineralogical and morphological characterisation of road dust and associated health risks. *Int. J. Environ. Res. Public Health* **2020**, *17*, 1563. [[CrossRef](#)]
52. Adamiec, E. Road environments: Impact of metals on human health in heavily congested cities in Poland. *Int. J. Environ. Res. Public Health* **2017**, *14*, 697. [[CrossRef](#)] [[PubMed](#)]